一般相対論の数値計算手法

近畿大セミナー
2011/12/9-10

真貝寿明　Hisa-aki Shinkai
大阪工業大学情報科学部　shinkai@is.oit.ac.jp

Contents

Procedure of the Standard Numerical Relativity

■ 3+1 (ADM) formulation

Need to solve elliptic PDEs
-- Conformal approach
-- Thin-Sandwich approach

■ Preparation of the Initial Data

- ◆ Assume the background metric
- ◆ Solve the constraint equations

■ Time Evolution

```
do time=1, time_end
```

- ◆ Specify the slicing condition
- ◆ Evolve the variables
- ◆ Check the accuracy
- ◆ Extract physical quantities

```
end do
```

Initial Data Construction Problem

Prepare all metric and matter components by solving the two constraints:

- The Hamiltonian constraint equation

$$^{(3)}R + (\mathrm{tr}K)^2 - K_{ij}K^{ij} = 2\kappa\rho + 2\Lambda \tag{1}$$

- The momentum constraint equations

$$D_j(K^{ij} - \gamma^{ij}\mathrm{tr}K) = \kappa J^i \tag{2}$$

We have 12 variables (γ_{ij}, K_{ij}) to fix, but only 4 constraints. ... How?

共形変換法 Conformal Approach – York-ÓMurchadha (1974)

N.ÓMurchadha and J.W.York Jr., Phys. Rev. **D 10**, 428 (1974)

この世 あの世

The key idea is solution $\gamma_{ij} = \psi^4 \hat{\gamma}_{ij}$ trial metric.

- the decomposition of K_{ij},

$$K_{ij} \Rightarrow \begin{cases} \mathrm{tr}K = \gamma^{ij} K_{ij} & \text{trace part} \\ A_{ij} = K_{ij} - \frac{1}{3}\gamma_{ij}\mathrm{tr}K & \text{trace-free part} \end{cases}$$

- conformal transformations:

$$\begin{aligned} \gamma_{ij} &= \psi^4 \hat{\gamma}_{ij}, & \gamma^{ij} &= \psi^{-4} \hat{\gamma}^{ij}, \\ A^{ij} &= \psi^{-10} \hat{A}^{ij}, & A_{ij} &= \psi^{-2} \hat{A}_{ij}, \\ \rho &= \psi^{-n} \hat{\rho}, & J^i &= \psi^{-10} \hat{J}^i, \end{aligned}$$

- we suppose

$$\mathrm{tr}K = \hat{\mathrm{tr}}\hat{K}, \quad \mathrm{tr}A = \hat{\mathrm{tr}}\hat{A} = 0.$$

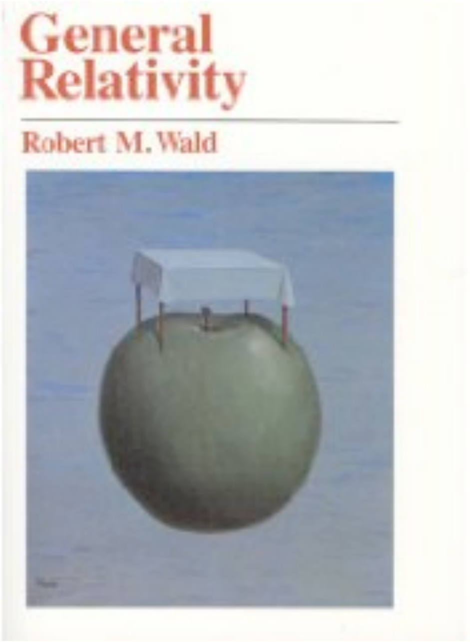

Appendix C

- we then get

$$\Gamma^i{}_{jk} = \hat{\Gamma}^i{}_{jk} + 2\psi^{-1}(\delta^i{}_j \hat{D}_k\psi + \delta^i{}_k \hat{D}_j\psi - \hat{\gamma}_{jk}\hat{\gamma}^{im}\hat{D}_m\psi),$$
$$R = \psi^{-4}\hat{R} - 8\psi^{-5}\hat{\Delta}\psi.$$

where $\hat{\Delta} = \hat{\gamma}^{jk}\hat{D}_j\hat{D}_k$ and $\hat{R} = R(\hat{\gamma})$, and also $D_j A^{ij} = \psi^{-10}\hat{D}_j\hat{A}^{ij}$.

- decompose $\hat{A}^{ij}$ to transverse-traceless (TT) part and longitudinal part:

$$\hat{A}^{ij} = \underbrace{\hat{A}^{ij}_{TT}}_{\text{divergence-free}} + \underbrace{(\hat{\mathbf{l}}W)^{ij}}_{\text{longitudinal}},$$

$$\hat{D}_j\hat{A}^{ij}_{TT} = 0, \quad \text{tr}\hat{A}_{TT} = 0, \quad \text{and} \quad (\hat{\mathbf{l}}W)^{ij} = \hat{D}^i W^j + \hat{D}^j W^i - \frac{2}{3}\hat{\gamma}^{ij}\hat{D}_k W^k.$$

- Using these terms, we can write

$$\hat{D}_j\hat{A}^{ij} = \hat{D}_j(\hat{\mathbf{l}}W)^{ij} \equiv (\hat{\Delta}_{\mathbf{l}}W)^i = (\hat{\Delta}W)^i + (1/3)\hat{D}^i(\hat{D}_j W^j) + \hat{R}^i{}_j W^j.$$

With above transformation, the two constraints becomes

- The Hamiltonian constraint equation

$$8\hat{\Delta}\psi = \hat{R}\psi - (\hat{A}_{ij}\hat{A}^{ij})\psi^{-7} + [\frac{2}{3}(\text{tr}K)^2 - 2\Lambda]\psi^5 - 16\pi G\hat{\rho}\psi^{5-n}$$

- The momentum constraint equations

$$\hat{\Delta}W^i + \frac{1}{3}\hat{D}^i\hat{D}_k W^k + \hat{R}^i{}_k W^k = \frac{2}{3}\psi^6\hat{D}^i\text{tr}K + 8\pi G\hat{J}^i$$

Conformal approach (York-ÓMurchadha, 1974)

One way to set up the metric and matter components $(\gamma_{ij}, K_{ij}, \rho, J^i)$ so as to satisfy the constraints:

1. Specify metric components $\hat{\gamma}_{ij}$, tr$K$, $\hat{A}_{ij}^{TT}$, and matter distribution $\hat{\rho}$, $\hat{J}$ in the conformal frame.

2. Solve the next equations for $(\psi,\ W^i)$

$$8\hat{\Delta}\psi = \hat{R}\psi - (\hat{A}_{ij}\hat{A}^{ij})\psi^{-7} + [(2/3)(\mathrm{tr}K)^2 - 2\Lambda]\psi^5 - 16\pi G\hat{\rho}\psi^{5-n} \quad (1)$$

$$\hat{\Delta}W^i + (1/3)\hat{D}^i\hat{D}_kW^k + \hat{R}^i{}_kW^k = (2/3)\psi^6\hat{D}^i\mathrm{tr}K + 8\pi G\hat{J}^i \quad (2)$$

   where $\hat{A}^{ij} = \hat{A}^{ij}_{TT} + \hat{D}^iW^j + \hat{D}^jW^i - (2/3)\hat{\gamma}^{ij}\hat{D}_kW^k$.

3. Apply the inverse conformal transformation and get the metric and matter components $\gamma_{ij},\ K_{ij},\ \rho,\ J^i$ in the physical frame:

$$\begin{aligned}
\gamma_{ij} &= \psi^4\hat{\gamma}_{ij}, \\
K_{ij} &= \psi^{-2}[\hat{A}_{ij}^{TT} + (\hat{\mathbf{l}}W)_{ij}] + (1/3)\psi^4\hat{\gamma}_{ij}\mathrm{tr}K, \\
\rho &= \psi^{-n}\hat{\rho}, \\
J^i &= \psi^{-10}\hat{J}^i
\end{aligned}$$

Comments

- Using the idea of conformal rescaling, we have a way to fix 12 components of (γ_{ij}, K_{ij}) that satisfy 4 constraints.
- The Hamiltonian constraint, (3), is a non-linear elliptic equation for ψ, so that we have to solve it by an iterative method.
- The momentum constraints, (3), are PDEs for W^i and coupled with (3). If we assume tr$K = 0$, then two constraints are decoupled. Normally people assume $\boxed{\mathrm{tr}K = 0}$ (maximal slicing condition) or $(\mathrm{tr}K)$ =const. (constant mean curvature slicing) for this purpose.
- For simplicity, people assume the background metric $\hat{\gamma}_{ij}$ is conformally flat $\boxed{\hat{\gamma}_{ij} = \delta_{ij}}$. The physical appropriateness of conformal flatness is often debatable.
- Two freedom of $\hat{A}^{TT}_{ij}$ corresponds to the one of gravitational wave. However, there have been no systematic discussion how to specify them, except applying tensor harmonics in a linearized situation.

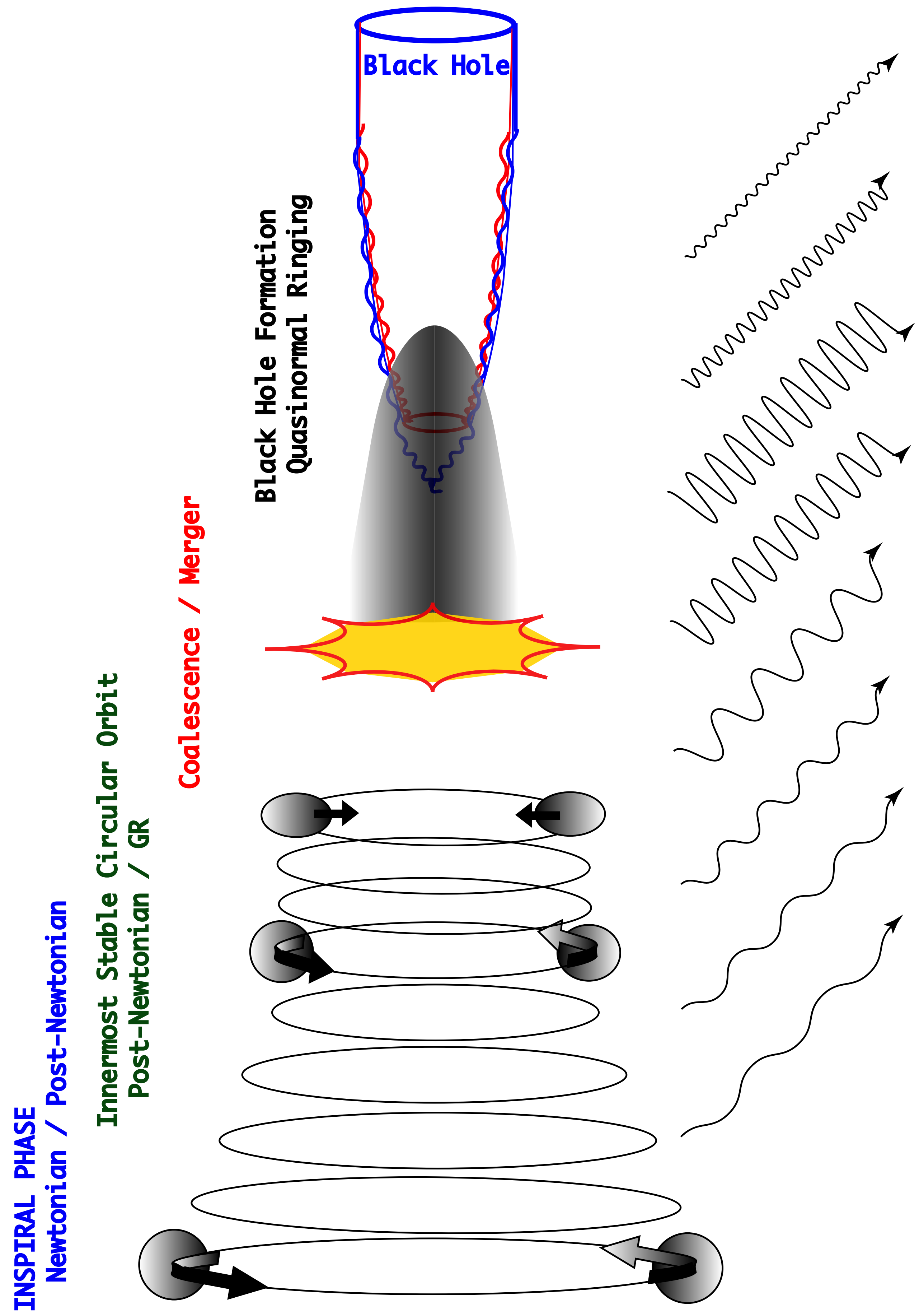
Black Hole
Black Hole Formation
Quasinormal Ringing
Coalescence / Merger
Innermost Stable Circular Orbit
Post-Newtonian / GR
INSPIRAL PHASE
Newtonian / Post-Newtonian

Numerical procedures – Several tips

Solving the Hamiltonian constraint

$$8\hat{\Delta}\psi = \hat{R}\,\psi - \hat{K}^{TF}_{ij}\hat{K}^{ij}_{TF}\,\psi^{-7} + \frac{2}{3}\hat{K}^2\,\psi^5 - 16\pi G\,\hat{\rho}\,\psi^{5-n}$$

1. Solve the non-linear equation directly.
2. Solve the linearized equation $\psi = \psi_0 + \delta\psi$ iteratively

$$\begin{aligned} 8\hat{\Delta}\psi &= E\,\psi + F\,\psi^{-7} + G\,\psi^5 + H\,\psi^{-3} + I\,\psi^{-1} \\ &= [E - 7F\psi_0^{-8} + 5G\psi_0^4 - 3H\psi_0^{-4} - 2I\psi_0^{-2}]\,\psi + [8F\psi_0^{-7} - 4G\psi_0^5 + 4H\psi_0^{-3} + 2I\psi_0^{-1}] \end{aligned}$$

Under an appropriate boundary condition, such as Robin BC $\psi = 1 + const./r$, or Dirichlet BC $\psi = 1 + M_{total}/2r$.

楕円型偏微分方程式の数値解法は，境界条件の設定が命

3+1次元空間なら，漸近的平坦は， $\psi = 1 + \dfrac{C}{r}$

4+1次元空間なら， $\psi = 1 + \dfrac{C}{r^2}$

Solving the momentum constraints

$$(\Delta W)^i + \frac{1}{3}D^i D_j W^j + R^i{}_j W^j - \frac{2}{3}\psi^6 \hat{D}^i K = 8\pi G \hat{J}^i$$

1. Solve the non-linear equations directly

2. Bowen's method for conformally flat case [GRG14(1982)1183]
   Under the $(\nabla^i K = 0)$ condition,

$$\Delta W^i + \frac{1}{3}\nabla^i \nabla_j W^j = 8\pi S^i.$$

By introducing a decomposition of W^i into vector and gradient terms $W^i = V^i - \frac{1}{4}\nabla^i\theta$,

$$\begin{aligned} \Delta V^i &= 8\pi S^i, \\ \Delta\theta &= \nabla_i V^i, \end{aligned}$$

If the source is of finite extent, then the the asymptotic behavior of V^i and θ are given by

$$\begin{aligned} V^i &= -2\sum_{l=0}^{\infty} Q^{ij_1\cdots j_l} n_{j_1}\cdots n_{j_l}\frac{1}{r^{l+1}}, \\ \theta &= -\sum_{l=1}^{\infty} Q^{\{ij_1\cdots j_{l-1}\}} n_i n_{j_1}\cdots n_{j_{l-1}}\frac{1}{r^{l-1}} + \sum_{l=0}^{\infty}\frac{2(l+1)}{(2l+1)(2l+3)} Q_k^{kj_1\cdots j_l} n_{j_1}\cdots n_{j_l}\frac{1}{r^{l+1}} + \sum_{l=1}^{\infty}\frac{2l-1}{2l+1} M^{\{ij_1\cdots j_{l-1}\}} n_i n_{j_1}\cdots n_{j_{l-1}}\frac{1}{r^{l+1}} \end{aligned}$$

where $n^i = x^i r^{-1}$ in the Cartesian cordinate, the multipoles Q and M are defined as

$$\begin{aligned} Q^{ij_1\cdots j_l} &\equiv \frac{(2l-1)!!}{l!}\int S^i(\mathbf{r}) x^{\{j_1}x^{j_2}\cdots x^{j_l\}} dV, \\ M^{ij_1\cdots j_l} &\equiv \frac{(2l-1)!!}{l!}\int r^2 S^i(\mathbf{r}) x^{\{j_1}x^{j_2}\cdots x^{j_l\}} dV, \end{aligned}$$

and where brackets denote the completely symmetric trace-free part

$$Z^{\{ij_1\cdots j_l\}} = Z^{(ij_1\cdots j_l)} - \frac{l}{2l+1} Z_k^{k(j_1\cdots j_{l-1}}\delta^{j_l i)}$$

Conformal Approach to solve constraints : Eqs. for Initial Data construction

- We generalized the Conformal approach by York and ÓMurchadha (1974) to N-dim & for Gauss-Bonnet gravity.
- Conformal transformation

solution $\gamma_{ij} = \psi^{2m}\hat{\gamma}_{ij} \quad \gamma^{ij} = \psi^{-2m}\hat{\gamma}^{ij}$ trial metric

this gives

$$R = \psi^{-2m}\Big\{\hat{R} - 2(N-1)m\psi^{-1}(\hat{D}^a\hat{D}_a\psi) + (N-1)\big[2-(N-2)m\big]m\psi^{-2}(\hat{D}\psi)^2\Big\},$$

$$R_{ij} = \hat{R}_{ij} - m\hat{\gamma}_{ij}\psi^{-1}\hat{D}_a\hat{D}^a\psi - (N-2)m\psi^{-1}\hat{D}_i\hat{D}_j\psi + (N-2)m(m+1)\psi^{-2}\hat{D}_i\psi\hat{D}_j\psi - m\big[(N-2)m-1\big]\psi^{-2}(\hat{D}\psi)^2\hat{\gamma}_{ij},$$

$$R_{ijkl} = \psi^{2m}\Big\{\hat{R}_{ijkl} + m\psi^{-1}\hat{\gamma}_{il}\big[\hat{D}_j\hat{D}_k\psi - (m+1)\psi^{-1}\hat{D}_j\psi\hat{D}_k\psi\big] - m\psi^{-1}\hat{\gamma}_{ik}\big[\hat{D}_j\hat{D}_l\psi - (m+1)\psi^{-1}\hat{D}_j\psi\hat{D}_l\psi\big]$$
$$+ m\psi^{-1}\hat{\gamma}_{jk}\big[\hat{D}_i\hat{D}_l\psi - (m+1)\psi^{-1}\hat{D}_i\psi\hat{D}_l\psi\big] - m\psi^{-1}\hat{\gamma}_{jl}\big[\hat{D}_i\hat{D}_k\psi - (m+1)\psi^{-1}\hat{D}_i\psi\hat{D}_k\psi\big] + m^2\psi^{-2}(\hat{D}\psi)^2(\hat{\gamma}_{il}\hat{\gamma}_{jk} - \hat{\gamma}_{ik}\hat{\gamma}_{jl})\Big\}.$$

- Decompose the extrinsic curvature K_{ij} as $K_{ij} \equiv A_{ij} + \frac{1}{N}\gamma_{ij}K$, and assume

$$A_{ij} = \psi^{\ell}\hat{A}_{ij}, \quad A^{ij} = \psi^{\ell-4m}\hat{A}^{ij},$$
$$K = \psi^{\tau}\hat{K}$$

- When matter exists, define also the conformal transformation

$$\rho = \psi^{-p}\hat{\rho}, \qquad J^i = \psi^{-q}\hat{J}^i$$

Hamiltonian constraint

$$\begin{aligned}&2(N-1)m\hat{D}_a\hat{D}^a\psi-(N-1)[2-(N-2)m]m(\hat{D}\psi)^2\psi^{-1}\\&\quad=\hat{R}\psi-\frac{N-1}{N}\varepsilon\psi^{2m+2\tau+1}\hat{K}^2+\varepsilon\psi^{-2m+2\ell+1}\hat{A}_{ab}\hat{A}^{ab}+2\varepsilon\kappa^2\hat{\rho}\psi^{-p}-2\hat{\Lambda}\\&\qquad+\alpha_{GB}\left(M^2-4M_{ab}M^{ab}+M_{abcd}M^{abcd}\right)\psi^{2m+1}.\end{aligned}\qquad(14)$$

$$\begin{aligned}\hat{\Theta}&=\left(M^2-4M_{ab}M^{ab}+M_{abcd}M^{abcd}\right)\\&=(N-3)m\psi^{-4m}\Big\{4(N-2)m\psi^{-2}\Big[(\hat{D}_a\hat{D}^a\psi)^2-\hat{D}_a\hat{D}_b\psi\hat{D}^a\hat{D}^b\psi\Big]-4\psi^{-1}\Big[\hat{M}-(N-2)\big[(N-3)m-2\big]m\psi^{-2}\hat{D}_a\psi\hat{D}^a\psi\Big]\hat{D}_a\hat{D}^a\psi\\&\qquad+8\psi^{-1}\Big[\hat{M}^{ab}+(N-2)m(m+1)\psi^{-2}\hat{D}^a\psi\hat{D}^b\psi\Big]\hat{D}_a\hat{D}_b\psi+(N-1)_2m^2\big[(N-4)m-4\big]\psi^{-4}(\hat{D}_a\psi\hat{D}^a\psi)^2-2\psi^{-2}\big[(N-4)m-2\big]\hat{M}\hat{D}_c\psi\hat{D}^c\psi\\&\qquad-8(m+1)\psi^{-2}\hat{M}^{ab}\hat{D}_a\psi\hat{D}_b\psi\Big\}+\psi^{-4m}(\hat{\Upsilon}^2-4\hat{\Upsilon}_{ab}\hat{\Upsilon}^{ab}+\hat{\Upsilon}_{abcd}\hat{\Upsilon}^{abcd}),\end{aligned}$$

where $\hat{\Upsilon}=\hat{R}-\varepsilon\left[\frac{N-1}{N}\psi^{2m+2\tau}\hat{K}^2-\psi^{2\ell-2m}\hat{A}_{ab}\hat{A}^{ab}\right]$, $\hat{\Upsilon}_{ij}=\hat{R}_{ij}-\varepsilon\left[\frac{N-1}{N^2}\psi^{2m+2\tau}\hat{\gamma}_{ij}\hat{K}^2+\frac{N-2}{N}\psi^{\ell+\tau}\hat{K}\hat{A}_{ij}-\psi^{2\ell-2m}\hat{A}_{ia}\hat{A}^a{}_j\right]$,

$$\hat{\Upsilon}_{ijkl}=\hat{R}_{ijkl}-\varepsilon\left[\frac{1}{N^2}\psi^{2m+2\tau}(\hat{\gamma}_{ik}\hat{\gamma}_{jl}-\hat{\gamma}_{il}\hat{\gamma}_{jk})\hat{K}^2+\frac{1}{N}\psi^{\ell+\tau}(\hat{A}_{ik}\hat{\gamma}_{jl}-\hat{A}_{il}\hat{\gamma}_{jk}+\hat{A}_{jl}\hat{\gamma}_{ik}-\hat{A}_{jk}\hat{\gamma}_{il})+\psi^{2\ell-2m}(\hat{A}_{ik}\hat{A}_{jl}-\hat{A}_{il}\hat{A}_{jk})\right].$$

(A) If we specify $\tau=\ell-2m$ and $m=2/(N-2)$, then (14) becomes

$$\frac{4(N-1)}{N-2}\hat{D}_a\hat{D}^a\psi=\hat{R}\psi-\varepsilon\psi^{2\ell+1-4/(N-2)}\left(\hat{K}^2-\hat{K}_{ab}\hat{K}^{ab}\right)+2\varepsilon\kappa^2\hat{\rho}\psi^{-p}-2\hat{\Lambda}+\alpha_{GB}\hat{\Theta}\psi^{1+4/(N-2)}.\qquad(15)$$

(B) If we specify $\tau=0$ and $m=2/(N-2)$, then (14) becomes

$$\frac{4(N-1)}{N-2}\hat{D}_a\hat{D}^a\psi=\hat{R}\psi-\varepsilon\frac{N-1}{N}\psi^{1+4/(N-2)}\hat{K}^2+\varepsilon\psi^{2\ell+1-4/(N-2)}\hat{A}_{ab}\hat{A}^{ab}+2\varepsilon\kappa^2\hat{\rho}\psi^{-p}-2\hat{\Lambda}+\alpha_{GB}\hat{\Theta}\psi^{1+4/(N-2)}.\qquad(16)$$

Momentum constraint

- Introduce the TT part and the longitudinal part of $\hat{A}^{ij}$, and its vector potential as

$$\hat{D}_j\hat{A}^{ij}_{TT}=0,\quad \hat{A}^{ij}_{L}=\hat{A}^{ij}-\hat{A}^{ij}_{TT},\quad \hat{A}^{ij}_{L}=\hat{D}^iW^j+\hat{D}^jW^i-\frac{2}{N}\hat{\gamma}^{ij}\hat{D}_kW^k.$$

- Conformal transformations: $D_jA_i{}^j=\psi^{\ell-2m}\Big\{\hat{D}_j\hat{A}_i{}^j+\psi^{-1}[\ell+m(N-2)]\hat{A}_i{}^j\hat{D}_j\psi\Big\}$

$$\begin{aligned}&\hat{D}_a\hat{D}^aW_i+\frac{N-2}{N}\hat{D}_i\hat{D}_kW^k+\hat{R}_{ik}W^k\\&+\psi^{-1}[\ell+(N-2)m]\Big(\hat{D}^aW^b+\hat{D}^bW^a-\frac{2}{N}\hat{\gamma}^{ab}\hat{D}_kW^k\Big)\hat{\gamma}_{bi}\hat{D}_a\psi\\&-\psi^{2m-\ell}\frac{N-1}{N}\hat{D}_i(\psi^\tau\hat{K})+\psi^{2m-\ell}2\alpha_{GB}\hat{\Xi}_i=\kappa^2\psi^{4m-\ell-q}\hat{J}_i\quad \text{(See next page for } \hat{\Xi}_i\text{.)}\end{aligned}\tag{17}$$

(A) If we specify $\tau=\ell-2m$ and $m=2/(N-2)$, then (17) becomes

$$\begin{aligned}&\hat{D}_a\hat{D}^aW_i+\frac{N-2}{N}\hat{D}_i\hat{D}_kW^k+\hat{R}_{ik}W^k+\psi^{-1}(\ell+2)\Big(\hat{D}^aW^b+\hat{D}^bW^a-\frac{2}{N}\hat{\gamma}^{ab}\hat{D}_kW^k\Big)\hat{\gamma}_{bi}\hat{D}_a\psi\\&-\frac{N-1}{N}\left[\Big(\ell-\frac{4}{N-2}\Big)(\hat{D}_i\psi)\hat{K}+\hat{D}_i\hat{K}\right]+\psi^{-\ell+4/(N-2)}2\alpha_{GB}\hat{\Xi}_i=\kappa^2\psi^{8/(N-2)-\ell-q}\hat{J}_i\end{aligned}\tag{18}$$

(B) If we specify $\tau=0$ and $m=2/(N-2)$, then (17) becomes

$$\begin{aligned}&\hat{D}_a\hat{D}^aW_i+\frac{N-2}{N}\hat{D}_i\hat{D}_kW^k+\hat{R}_{ik}W^k+\psi^{-1}(\ell+2)\big[\hat{D}^aW^b+\hat{D}^bW^a-\frac{2}{N}\hat{\gamma}^{ab}\hat{D}_kW^k\big]\hat{\gamma}_{bi}\hat{D}_a\psi\\&-\psi^{4/(N-2)-\ell}\frac{N-1}{N}\hat{D}_i\hat{K}+\psi^{4/(N-2)-\ell}2\alpha_{GB}\hat{\Xi}_i=\kappa^2\psi^{8/(N-2)-\ell-q}\hat{J}_i\end{aligned}\tag{19}$$

$$
\begin{aligned}
\Xi_i = {} & \psi^{\ell-4m}\Big\{\hat{R} - 2(N-3)m\psi^{-1}\hat{D}_b\hat{D}^b\psi - (N-3)m\big[(N-4)m+2\big]\psi^{-2}\hat{D}_b\psi\hat{D}^b\psi - \frac{N^2-3N+4}{N^2}\varepsilon\psi^{+2m+2\tau}\hat{K}^2 - \varepsilon\psi^{2\ell-2m}\hat{A}_{bc}\hat{A}^{bc}\Big\}\hat{D}_a\hat{A}^a{}_i \\
& + \psi^{\ell-4m}\Big\{-2\hat{R}^b{}_i + 2(N-3)m\psi^{-1}\hat{D}^b\hat{D}_i\psi - 2(N-3)m(m+1)\psi^{-2}\hat{D}_i\psi\hat{D}^b\psi + \frac{2(N-3)}{N}\varepsilon\psi^{\ell+\tau}\hat{K}\hat{A}_i{}^b - 2\varepsilon\psi^{2\ell-2m}\hat{A}_i{}^c\hat{A}_c{}^b\Big\}\hat{D}_a\hat{A}^a{}_b \\
& + \psi^{\ell-4m}\Big\{2\hat{R}^{ab} - 2(N-3)m\psi^{-1}\hat{D}^b\hat{D}^a\psi - 2(N-1)m(m+1)\psi^{-2}\hat{D}^a\psi\hat{D}^b\psi - \frac{2(N-3)}{N}\varepsilon\psi^{\ell+\tau}\hat{K}\hat{A}^{ab} + 2\varepsilon\psi^{2\ell-2m}\hat{A}^a{}_c\hat{A}^{cb}\Big\}\big(\hat{D}_i\hat{A}_{ab} - \hat{D}_a\hat{A}_{ib}\big) \\
& + 2\varepsilon\psi^{3\ell-6m}\hat{A}_i{}^a\hat{A}^{bc}\big(\hat{D}_a\hat{A}_{bc} - \hat{D}_b\hat{A}_{ac}\big) + \mathcal{R}_i + \mathcal{D}_i + \mathcal{A}^{(1)}\hat{D}_i\psi + \mathcal{A}^{(2)}\hat{D}_i\hat{K} + \mathcal{A}^{(3)}\hat{D}_a\psi\hat{A}^a{}_i \\
& - \frac{2(N-2)_3}{N^2}\varepsilon\psi^{\ell-2m+2\tau}\hat{K}(\hat{D}_a\hat{K} + \tau\psi^{-1}\hat{K}\hat{D}_a\psi)\hat{A}^a{}_i + \frac{2(N-3)}{N}\big[(N-4)m+2\ell+\tau\big]\varepsilon\psi^{2\ell-4m+\tau-1}\hat{K}\hat{D}_b\psi\hat{A}^b{}_a\hat{A}^a{}_i \\
& + \frac{2(N-3)}{N}\varepsilon\psi^{2\ell-4m+\tau}\hat{D}_b\hat{K}\hat{A}^b{}_a\hat{A}^a{}_i - 2\big[(N-6)m+3\ell\big]\varepsilon\psi^{3\ell-6m-1}\hat{D}_c\psi\hat{A}^c{}_b\hat{A}^b{}_a\hat{A}^a{}_i,
\end{aligned}
$$

where

$$
\begin{aligned}
\mathcal{R}_i = {} & \Big\{\big[(N-3)m+\ell\big]\psi^{\ell-4m-1}\hat{A}_i{}^a\hat{D}_a\psi - \frac{N-3}{N}\psi^{-2m+\tau}(\hat{D}_i\hat{K} + \tau\psi^{-1}\hat{K}\hat{D}_i\psi)\Big\}\hat{R} \\
& + \Big\{\frac{2(N-3)}{N}\tau\psi^{-2m+\tau-1}\hat{K}\hat{D}_a\psi + \frac{2(N-3)}{N}\psi^{-2m+\tau}\hat{D}_a\hat{K} - 2\big[(N-3)m+\ell\big]\psi^{\ell-4m-1}\hat{A}_a{}^b\hat{D}_b\psi\Big\}\hat{R}_i{}^a \\
& - 2(m-\ell)\psi^{\ell-4m-1}(\hat{A}_{ab}\hat{D}_i\psi - \hat{A}_{ib}\hat{D}_a\psi)\hat{R}^{ab} + 2(m-\ell)\psi^{\ell-4m-1}\hat{D}_a\psi\hat{A}_{bc}\hat{R}_i{}^{cab}, \\
\mathcal{D}_i = {} & \Big\{\frac{N^2-8N+11}{N}m\psi^{-2m+\tau-1}(\hat{D}_i\hat{K} + \tau\psi^{-1}\hat{K}\hat{D}_i\psi) - 2m\big[(N^2-6N+7)m + (N-3)\ell\big]\psi^{\ell-4m-2}\hat{D}_b\psi\hat{A}^b{}_i\Big\}\hat{D}_a\hat{D}^a\psi \\
& - \Big\{\frac{2(N-2)_3}{N}m\psi^{-2m+\tau-1}(\hat{D}_a\hat{K} + \tau\psi^{-1}\hat{K}\hat{D}_a\psi) - 2m\big[(N^2-4N+5)m + (N-2)(\ell-2)\big]\psi^{\ell-4m-2}\hat{D}_b\psi\hat{A}^b{}_a\Big\}\hat{D}^a\hat{D}_i\psi \\
& + 2(N-3)m(m-\ell)\psi^{\ell-4m-2}(\hat{A}_{ab}\hat{D}_i\psi - \hat{A}_{ia}\hat{D}_b\psi)\hat{D}^b\hat{D}^a\psi, \\
\mathcal{A}^{(1)} = {} & 2\Big\{-\frac{N-2}{N}m(m+1)\psi^{-2m+2\tau-2}(\hat{D}_a\hat{K} + \tau\psi^{-1}\hat{K}\hat{D}_a\psi)(\hat{D}^a\hat{K} + \tau\psi^{-1}\hat{K}\hat{D}^a\psi) \\
& \quad + \frac{(N-2)^2}{N}m(m+1)\psi^{-2m+\tau-2}\hat{D}_a\hat{K}\hat{D}^a\psi + \frac{N-2}{2N}m\big[(N^2-4N+5)m+2\big]\tau\psi^{-2m+\tau-3}\hat{K}\hat{D}_a\psi\hat{D}^a\psi \\
& \quad - (N-2)_3 m^2(m+1)\psi^{\ell-4m-3}\hat{D}^a\psi\hat{D}^b\psi\hat{A}_{ab} + \frac{N-3}{N}(m-\ell-\tau)\varepsilon\psi^{2\ell-4m+\tau-1}\hat{K}\hat{A}_{ab}\hat{A}^{ab} - (m-\ell)\varepsilon\psi^{3\ell-6m-1}\hat{A}_a{}^b\hat{A}_b{}^c\hat{A}_c{}^a\Big\}, \\
\mathcal{A}^{(2)} = {} & \frac{1}{N}\Big\{(N-2)_3 m\big[(N-3)m-2\big]\psi^{-2m+\tau-2}\hat{D}_a\psi\hat{D}^a\psi - \frac{(N-1)_2(N+1)}{N^2}\varepsilon\psi^{3\tau}\hat{K}^2 - (N-3)\varepsilon\psi^{2\ell-4m+\tau}\hat{A}_{ab}\hat{A}^{ab}\Big\}, \\
\mathcal{A}^{(3)} = {} & -m\big[(N-2)^2(N-5)m^2 + (N-2)_3(\ell-2)m + (N-1)(3\ell-2)\big]\psi^{\ell-4m-3}\hat{D}_a\psi\hat{D}^a\psi \\
& - \frac{1}{N^2}\big[(N-1)(N^2-8)m + (N^2-N+2)\ell\big]\varepsilon\psi^{\ell-2m+2\tau-1}\hat{K}^2 + \big[(N-6)m+3\ell\big]\varepsilon\psi^{3\ell-6m-1}\hat{A}_{ab}\hat{A}^{ab}.
\end{aligned}
$$

(A) Hamiltonian constraint

$$\frac{4(N-1)}{N-2}\hat{D}_a\hat{D}^a\psi = \hat{R}\psi - \varepsilon\psi^{2\ell+1-4/(N-2)}(\hat{K}^2 - \hat{K}_{ab}\hat{K}^{ab}) + 2\varepsilon\kappa^2\hat{\rho}\psi^{-p} - 2\hat{\Lambda} + \alpha_{GB}\hat{\Theta}\psi^{1+4/(N-2)}.$$

(A) momentum constraint

$$\hat{D}_a\hat{D}^a W_i + \frac{N-2}{N}\hat{D}_i\hat{D}_k W^k + \hat{R}_{ik}W^k + \psi^{-1}(\ell+2)\Big(\hat{D}^a W^b + \hat{D}^b W^a - \frac{2}{N}\hat{\gamma}^{ab}\hat{D}_k W^k\Big)\hat{\gamma}_{bi}\hat{D}_a\psi$$
$$-\frac{N-1}{N}\left[\Big(\ell - \frac{4}{N-2}\Big)(\hat{D}_i\psi)\hat{K} + \hat{D}_i\hat{K}\right] + \psi^{-\ell+4/(N-2)}2\alpha_{GB}\hat{\Xi}_i = \kappa^2\psi^{8/(N-2)-\ell-q}\hat{J}_i$$

Procedures to construct the initial hypersurface data $(\gamma_{ij}, K_{ij}, \rho, J^i)$

1. Give the initial assumption (trial values) for $\hat{\gamma}_{ij}$, tr$K$, $\hat{A}^{TT}_{ij}$ and $\hat{\rho}$, $\hat{J}$.
2. Solve above 2 equations for ψ and W^i.
3. inverse conformal transformations,

$$\gamma_{ij} = \psi^{4/(N-2)}\hat{\gamma}_{ij}, \quad K_{ij} = \psi^{\ell}[\hat{A}^{TT}_{ij} + (\hat{\mathbb{I}}W)_{ij}] + \frac{1}{N}\psi^{\ell-4/(N-2)}\hat{\gamma}_{ij}\mathrm{tr}K,$$
$$\rho = \psi^{-p}\hat{\rho}, \quad J^i = \psi^{-q}\hat{J}^i$$

Numerical Relativity – open issues — Box 1.2

0. How to foliate space-time

Cauchy $(3+1)$, Hyperboloidal $(3+1)$, characteristic $(2+2)$, or combined?

$\Rightarrow$ if the foliation is $(3+1)$, then $\cdots$

1. How to prepare the initial data

Theoretical:	Proper formulation for solving constraints? How to prepare realistic initial data? Effects of background gravitational waves? Connection to the post-Newtonian approximation?
Numerical:	Techniques for solving coupled elliptic equations? Appropriate boundary conditions?

2. How to evolve the data

Theoretical:	Free evolution or constrained evolution? Proper formulation for the evolution equations? $\Rightarrow$ see e.g. gr-qc/0209111 Suitable slicing conditions (gauge conditions)?
Numerical:	Techniques for solving the evolution equations? Appropriate boundary treatments? Singularity excision techniques? Matter and shock surface treatments? Parallelization of the code?

3. How to extract the physical information

Theoretical:	Gravitational wave extraction? Connection to other approximations?
Numerical:	Identification of black hole horizons? Visualization of simulations?

一般相対論の数値計算手法

近畿大セミナー
2011/12/9-10

真貝寿明 Hisa-aki Shinkai
大阪工業大学情報科学部 shinkai@is.oit.ac.jp

Contents

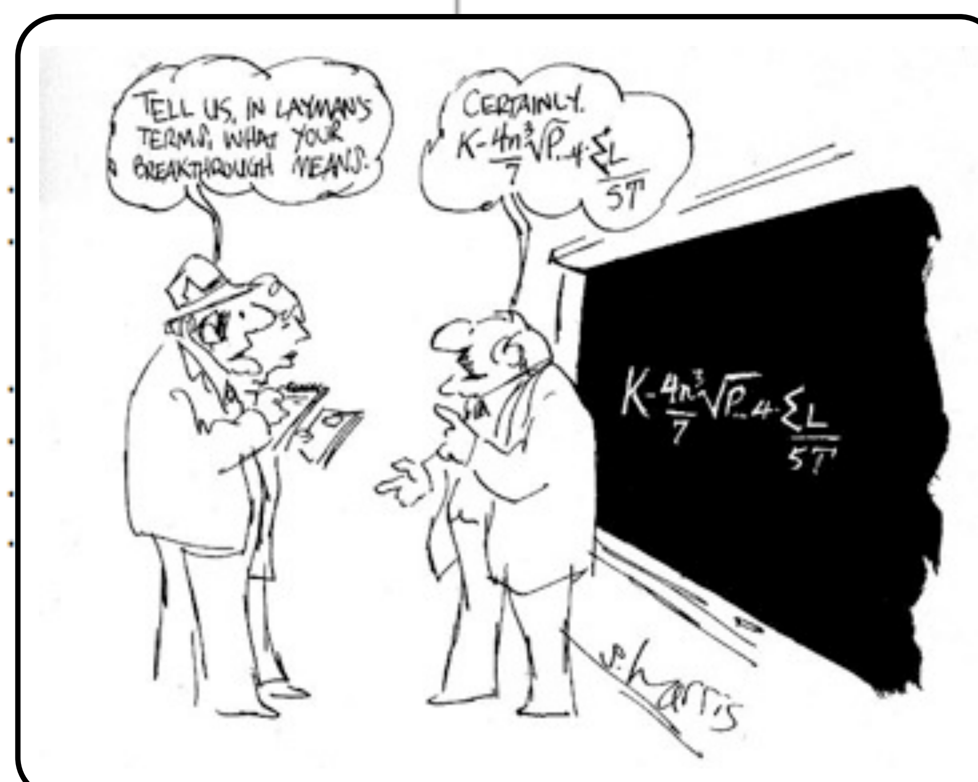

Procedure of the Standard Numerical Relativity

- 3+1 (ADM) formulation

- Preparation of the Initial Data
  - Assume the background metric
  - Solve the constraint equations

Need to solve elliptic PDEs
-- Conformal approach
-- Thin-Sandwich approach

- Time Evolution

do time=1, time_end
  - Specify the slicing conditions
  - Evolve the variables
  - Check the accuracy
  - Extract physical quantities

end do

singularity avoidance,
simplify the system,
GW extraction, ...

よい座標条件とは

How to choose gauge conditions?

The fundamental guidelines for fixing the lapse function α and the shift vector β_i:

- to avoid hitting the physical and coordinate singularity in its evolution.
- to make the system suitable for physical situation.
- to make the evolution system as simple as possible.
- to enable the gravitational wave extraction easy.

できるだけ特異点を回避できること．

できるだけ物理的な状況設定に近いものを再現すること

できるだけ単純なこと

重力波の抽出が簡単にできること（漸近的平坦であること）

Lapse 関数の候補

geodesic slice	$\alpha = 1$	GOOD	simple, easy to understand
		BAD	no singularity avoidance
harmonic slice	$\nabla_a \nabla^a x^b = 0$	GOOD	simplify eqs.,
		GOOD	easy to compare analytical investigations
		BAD	no singularity avoidance or coordinate pathologies
maximal slice	$K = 0$	GOOD	singularity avoidance
		BAD	have to solve an elliptic eq.
maximal slice (K-driver)	$\partial_t K = -c^2 K$	G&B	same with maximal slice,
		GOOD	easy to maintain $K = 0$
constant mean curvature	$K = const.$	G&B	same with maximal slice,
		GOOD	suitable for cosmological situation
polar slicing	$K_\theta^\theta + K_\varphi^\varphi = 0$, or $K = K_r^r$	GOOD	singularity avoidance in isotropic coord.
		BAD	trouble in Schwarzschild coord.
algebraic	$\alpha \sim \sqrt{\gamma}$, $\alpha \sim 1 + \log \gamma$	GOOD	easy to implement
		BAD	not avoiding singularity

Maximal slicing condition

- A singularity avoiding gauge condition.
- The name of 'maximal' comes from the fact that the deviation of the 3-volume $V = \int \sqrt{\gamma} d^3x$ along to the normal line becomes maximal when we set $K = 0$.
- This is simply written as

$$K = 0 \qquad \text{on} \quad \Sigma(t).$$

Practically, we solve

$$D^i D_i \alpha = \{ {}^{(3)}R + K^2 + 4\pi G(S - 3\rho_H) - 3\Lambda\}\alpha,$$

or by using the Hamiltonian constraint further,

$$D^i D_i \alpha = \{K_{ij} K^{ij} + 4\pi G(S + \rho_H) - \Lambda\}\alpha.$$

- This is an elliptic equation. When the curvature is strong (i.e. close to the appearance of a singularity), the RHS of equation become larger, hence the lapse becomes smaller. Therefore the foliation near the singularity evolves slowly.

Maximal Slicing Condition

In Schwarzschild geometry, K=0 slicing conditions allows us to evolve r=1.5M.

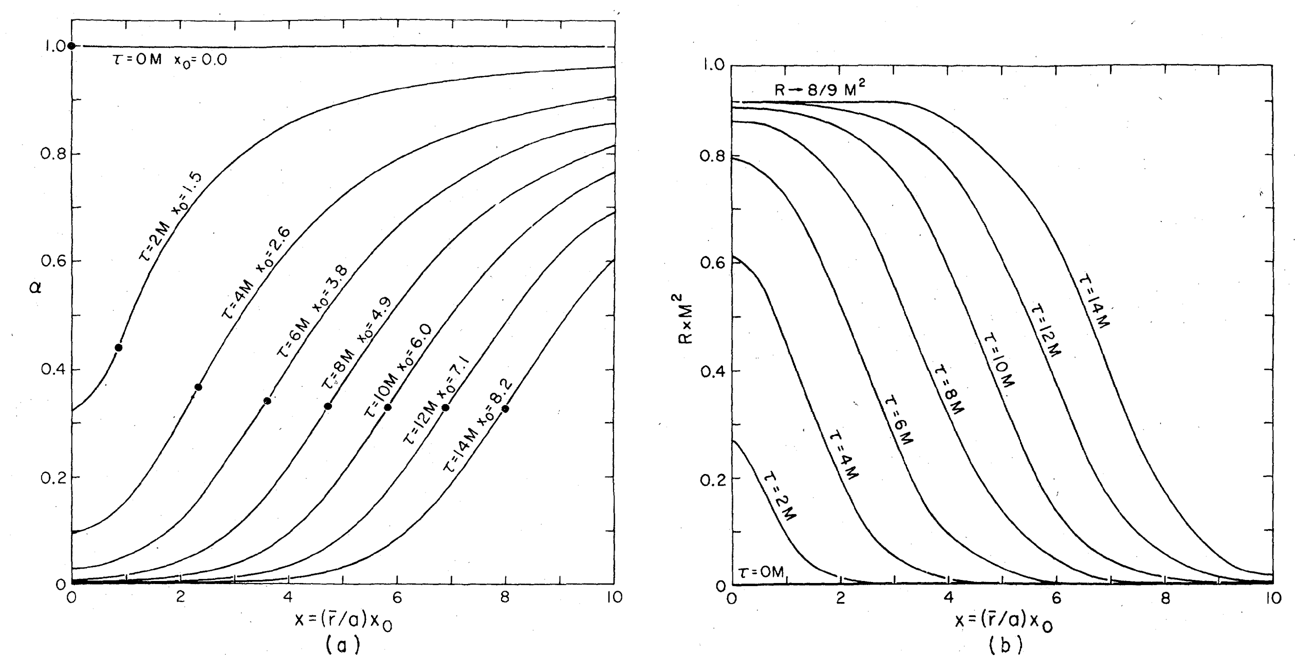

FIG. 3. (a) The spherically symmetric lapse function α is plotted versus the dimensionless radius $x \equiv (\bar{r}/a)x_0$ where $\bar{r}$ is the proper radial distance from the throat and x_0 and a are as defined by Eq. (3.7). These plots of $\alpha(x)$ are given for a series of time slices of the symmetric maximal slices of Schwarzschild-Kruskal spacetime studied by Estabrook *et al.* (Ref. 37). Notice the rapid collapse of the lapse near the throat at late times ($\tau \gtrsim 10M$). Time slices are labeled by the strength parameter x_0 and by proper time τ at a large finite distance (where we set $\alpha = 1$). The curves rise more rapidly than in Fig. 4 because this distance is not infinite. The location of the event horizon $r_{Sch} = 2M$ is denoted by a dot on each slice (see Eppley, Ref. 1). (b) For the same time slices as in (a), we plot the Ricci scalar $\mathcal{R}(x)$ of the three-metric of the slice. At $\tau = 0$, $\mathcal{R} = 0$ from the constraint equations. It grows in the strong-field region ($x \cong 0$) as time increases. This is what forces the lapses to zero in (a). At late times the central value of $\mathcal{R}$ goes to $8/9M^2$, the value of $\mathcal{R}$ for the hypercylinder $r_{Sch} = 3M/2$. The "effective radius" a [Eq. (3.7)] is found to grow linearly in time and be approximately the proper radial distance from the throat to the horizon in the time slice.

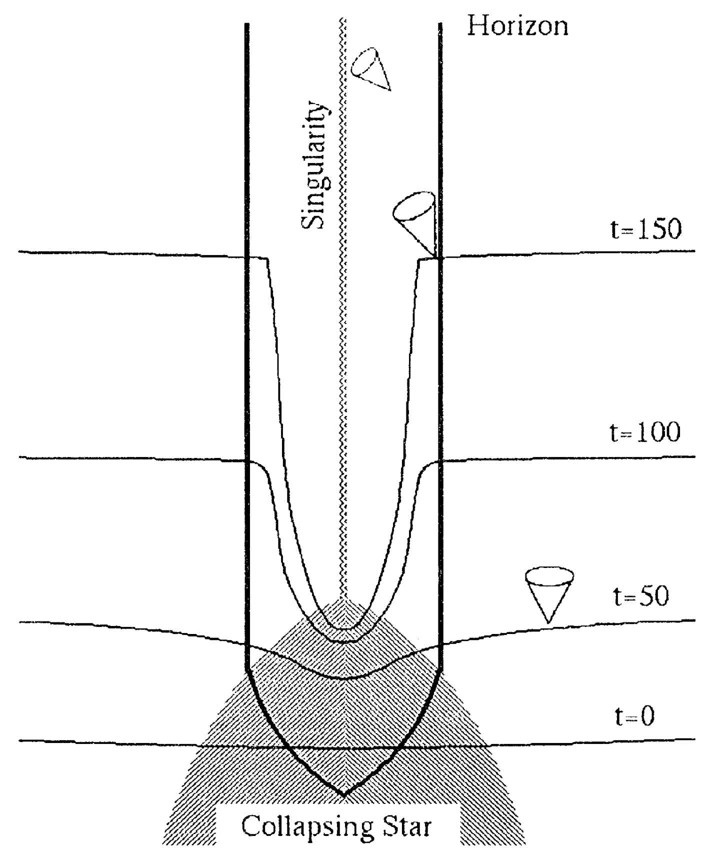

FIG. 1. A black hole spacetime diagram showing various singularity avoiding time slices that wrap up around the singularity inside the horizon. Such slicings allow short-term success in the numerical evolution of black holes, while at the same time causing pathological behavior that eventually dooms the calculation at late times.

Maximal slicing versus Harmonic slicing

A. Geyer and H. Herold, PRD31 (1995) 6182

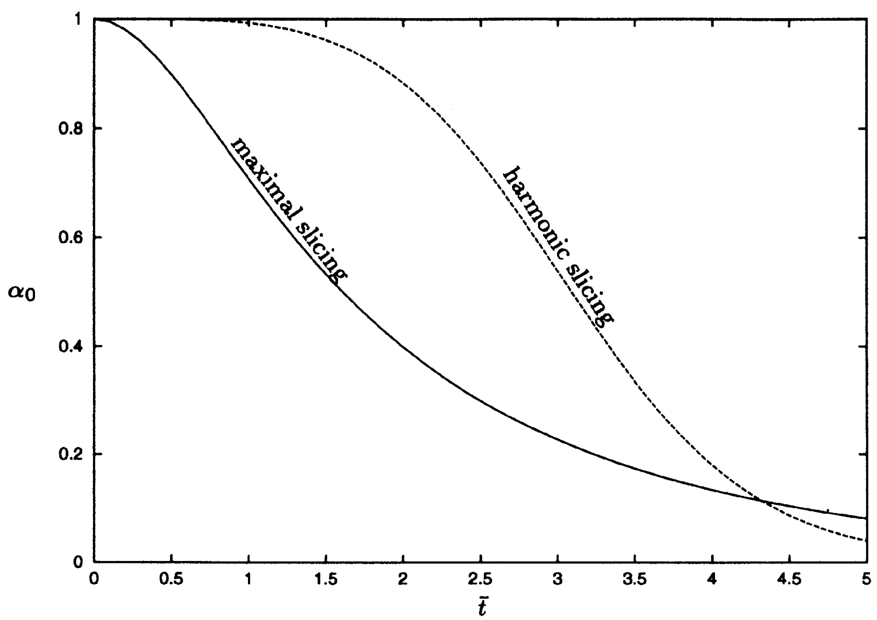

FIG. 2. The lapse on the $u = 0$ axis as a function of $\bar{t}$. For harmonic slicing the "collapse of the lapse" occurs at a later time $\bar{t}$ than in the case of maximal slicing.

Harmonic slicing hits singularity!

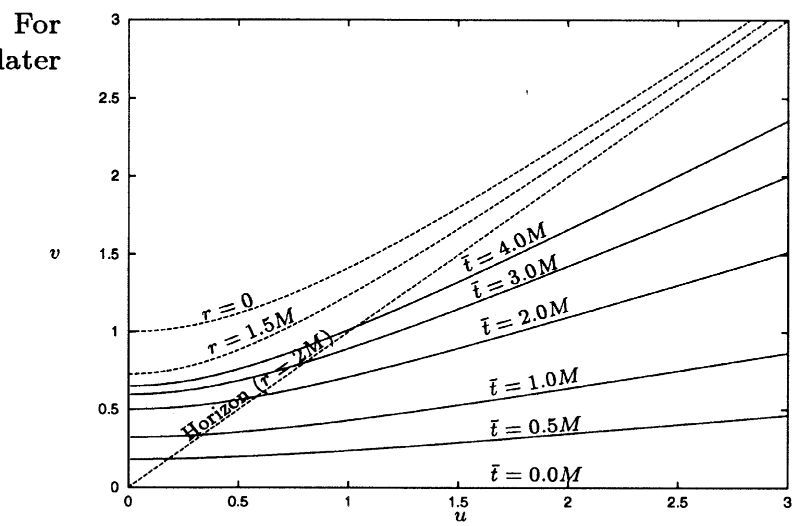

FIG. 1. Foliation of the Schwarzschild spacetime by maximal slices. The picture shows the projection of some $\bar{t}$ = const hypersurfaces in the Kruskal plane (compare [6]).

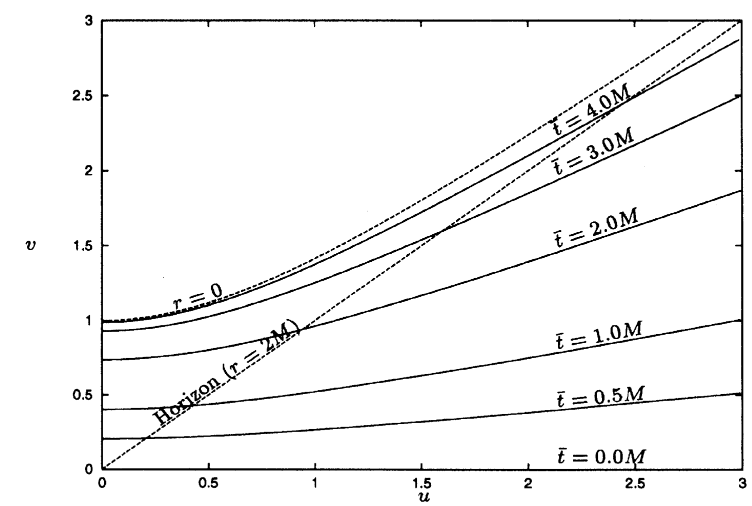

FIG. 3. Harmonic slices in the Schwarzschild spacetime constructed from the initial lapse $\alpha = 1$ on $v = 0$. Note that, in contrast with Fig. 1, the whole spacetime up to the singularity ($r = 0$) gets covered.

slicing conditions (lapse) α

Maximal slicing condition

$$K = 0 \quad \Leftrightarrow \quad \partial_t K = 0 \quad \Leftrightarrow$$

$$\triangle\alpha = \alpha(K_{ij}K^{ij} + \frac{2}{3}\kappa\rho + \frac{1}{3}\kappa S)$$

BC at far region $(\alpha - 1)r^2 = \text{const.} \quad \Leftrightarrow \quad \frac{\partial}{\partial x^i}\left[(\alpha - 1)r^2\right] = 0.$

" singularity avoidance "

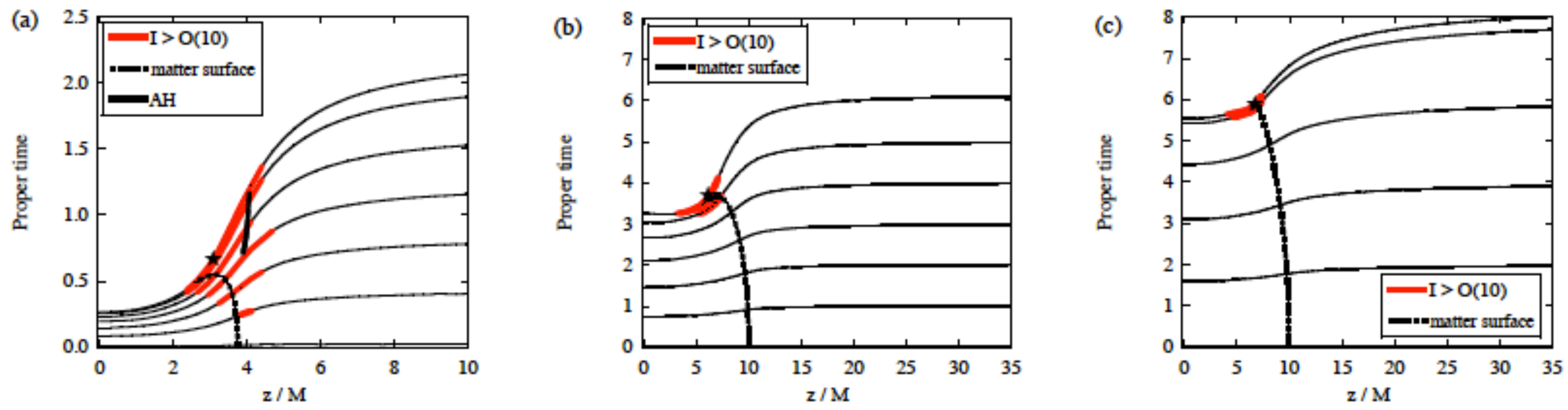

FIG. 4: The snapshots of the hypersurfaces on the z-axis in the proper-time versus coordinate diagram; (a) model 5DSβ, (b) model 5DSδ, and (c) model 4Dδ. The upper most hypersurface is the final data in numerical evolution. We also mark the matter surface and the location of AH if exist. The ranges with $\mathcal{I} \geq 10$ are marked with bold lines and peak value of $\mathcal{I}$ express by asterisks.

Lapse 関数の候補

geodesic slice	$\alpha = 1$	GOOD	simple, easy to understand
		BAD	no singularity avoidance
harmonic slice	$\nabla_a \nabla^a x^b = 0$	GOOD	simplify eqs.,
		GOOD	easy to compare analytical investigations
		BAD	no singularity avoidance or coordinate pathologies
maximal slice	$K = 0$	GOOD	singularity avoidance
		BAD	have to solve an elliptic eq.
maximal slice (K-driver)	$\partial_t K = -c^2 K$	G&B	same with maximal slice,
		GOOD	easy to maintain $K = 0$
constant mean curvature	$K = const.$	G&B	same with maximal slice,
		GOOD	suitable for cosmological situation
polar slicing	$K_\theta^\theta + K_\varphi^\varphi = 0$, or $K = K_r^r$	GOOD	singularity avoidance in isotropic coord.
		BAD	trouble in Schwarzschild coord.
algebraic	$\alpha \sim \sqrt{\gamma}$, $\alpha \sim 1 + \log \gamma$	GOOD	easy to implement
		BAD	not avoiding singularity

Shift 関数の候補

geodesic slice	$\beta^i = 0$	GOOD	simple, easy to understand
		BAD	too simple
minimal distortion	$\min \Sigma^{ij}\Sigma_{ij}$	GOOD	geometrical meaning
		BAD	elliptic eqs., hard to solve
minimal strain	$\min \Theta^{ij}\Theta_{ij}$	G&B	same with minimal distorsion

Minimal distortion condition, Minimal strain condition

L.Smarr and J.W.York,Jr., Phys. Rev. D **17**, 2529 (1978)

- Against the grid-streching, minimize the distortion in a global sense.
- The expansion tensor $\Theta_{\mu\nu}$: Let the coordinate-constant congruence $t_\mu = \alpha n_\mu + \beta_\mu$. Using the projection operator $\perp^a_b = \delta^a_b + n^a n_b$,

$$\Theta_{\mu\nu} = \perp \nabla_{(\nu} t_{\mu)} = -\alpha K_{\mu\nu} + \frac{1}{2} D_{(\mu}\beta_{\nu)}$$

- The distortion tensor Σ_{ij}:

$$\Sigma_{ij} = \Theta_{ij} - \frac{1}{3}\Theta\gamma_{ij} = -2\alpha\left(K_{ij} - \frac{1}{3}\gamma_{ij}K\right) + \frac{1}{2}\left(D_{(i}\beta_{j)} - \frac{1}{3}D^k\beta_k\right).$$

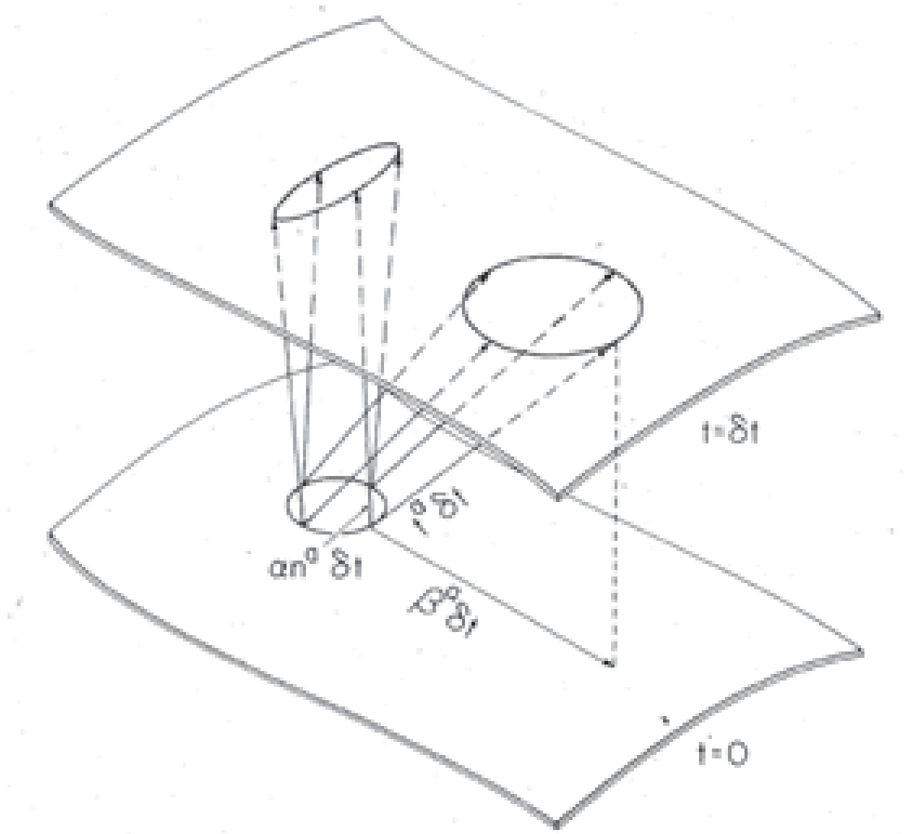

FIG. 7. This schematic diagram illustrates the use of the minimal-distortion shift vector to reduce coordinate shear. If a small sphere (here one spatial dimension is suppressed) is transported along the normal $\hat{n}^a$ to the next slice $\tau=\delta\tau$, it will be sheared into an ellipsoid. If the slicing is maximal, the volume will be preserved to first order. On the other hand, if a shift vector is also used, then some of this coordinate shear can be removed, although with the possible introduction of some change in volume.

The minimal distortion condition

- minimize $\Sigma_{ij}\Sigma^{ij}$

$$\delta S[\beta] = \delta\{\frac{1}{2}\int \Sigma_{ij}\Sigma^{ij} d^3x\} = 0.$$

- This condition can be written as $D^j\Sigma_{ij} = 0$, or

$$D^j D_j \beta_i + D^j D_i \beta_j - \frac{2}{3} D_i D_j \beta^j = D^j \left[2\alpha \left(K_{ij} - \frac{1}{3} trK\gamma_{ij} \right) \right],$$

or

$$\Delta\beta_i + \frac{1}{3} D_i (D^j \beta_j) + R_i^j \beta_j = D^j \left[2\alpha \left(K_{ij} - \frac{1}{3} trK\gamma_{ij} \right) \right],$$

where $\Delta = D^i D_i$.

The minimal strain condition

- minimize $\Theta^{ij}\Theta_{ij}$, similarly.

slicing conditions (shift) β^i

Minimal strain condition

$$\Theta_{\mu\nu} = \perp\nabla_{(\nu}t_{\mu)} = -\alpha K_{\mu\nu} + \frac{1}{2}D_{(\mu}\beta_{\nu)}, \quad \text{where} \quad t^\mu = \alpha n^\mu + \beta^\mu$$

$$D_j\Theta^{ij} = 0 \quad \Leftrightarrow \quad \triangle\beta^i + D^iD_j\beta^j + R_{ij}\beta^j = 2D^j(\alpha K_{ij}).$$

BC at far region $\beta r^2 = \text{const.} \quad \Leftrightarrow \quad \frac{\partial}{\partial x^i}\left[\beta r^2\right] = 0.$

" anti grid-stretching"

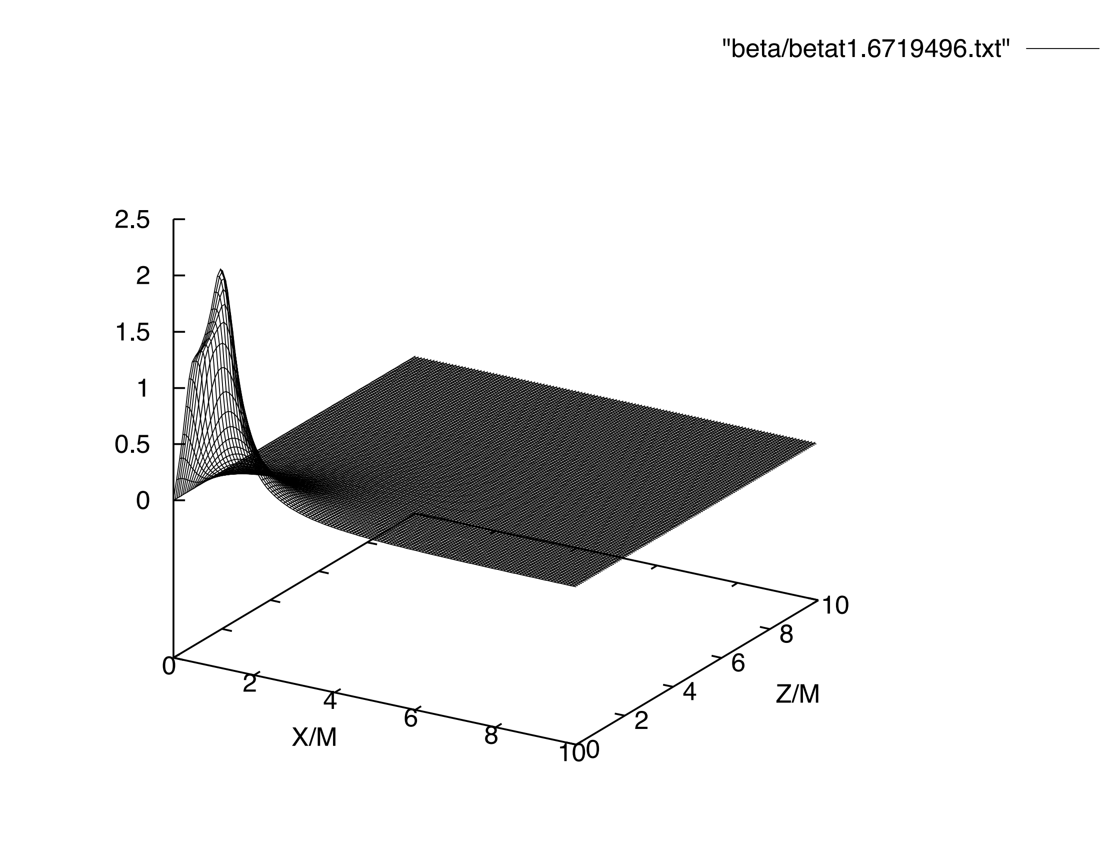

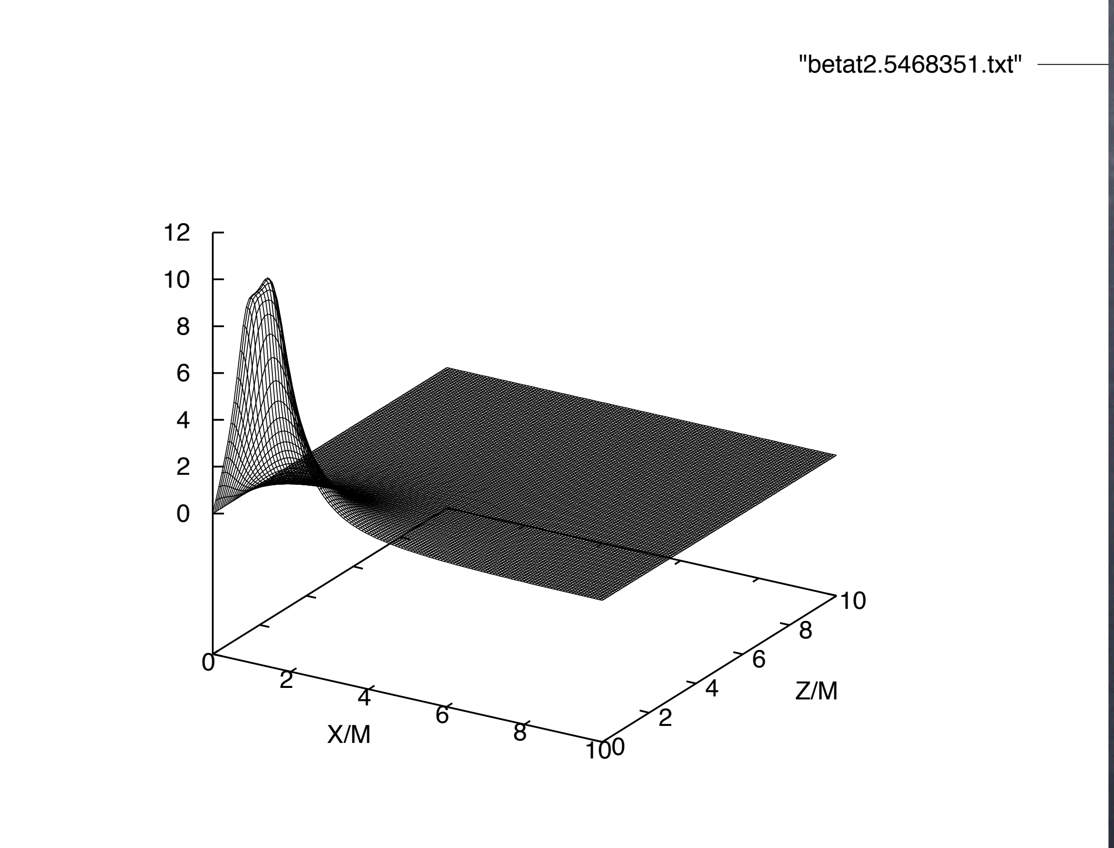

Procedure of the Standard Numerical Relativity

- 3+1 (ADM) formulation

- Preparation of the Initial Data
  - Assume the background metric
  - Solve the constraint equations

Need to solve elliptic PDEs
-- Conformal approach
-- Thin-Sandwich approach

- Time Evolution

do time=1, time_end
  - Specify the slicing conditions
  - Evolve the variables
  - Check the accuracy
  - Extract physical quantities
end do

singularity avoidance,
simplify the system,
GW extraction, ...

Procedure of the Standard Numerical Relativity

- 3+1 (ADM) formulation

- Preparation of the Initial Data
  - Assume the background metric
  - Solve the constraint equations

Need to solve elliptic PDEs
-- Conformal approach
-- Thin-Sandwich approach

- Time Evolution

  do time=1, time_end
  - Specify the slicing conditions
  - Evolve the variables
  - Check the accuracy
  - Extract physical quantities

  end do

singularity avoidance,
simplify the system,
GW extraction, ...

Robust formulation ?
-- modified ADM
-- hyperbolization
-- asymptotically constrained

一般相対論の数値計算手法

近畿大セミナー
2011/12/9-10

真貝寿明 Hisa-aki Shinkai
大阪工業大学情報科学部 shinkai@is.oit.ac.jp

Contents

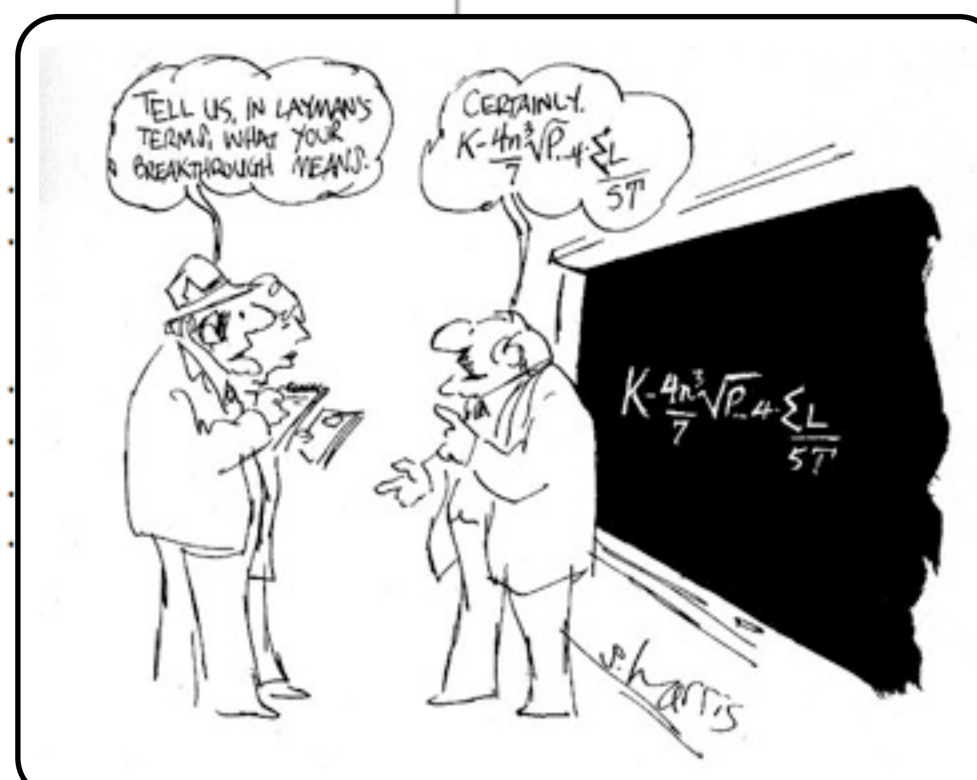

Numerical Simulations using Ashtekar variables

HS and G. Yoneda, Class. Quant. Grav. 17 (2000) 4799
Class. Quant. Grav. 18 (2001) 441

Objective

Compare numerical stability between three types of hyperbolic formulations.

Strategy

- plane symmetric, vacuum spacetime
  true freedom of gravitational wave of two polarized ($+$ and $\times$) modes.
- the same initial data ——— solve ADM constraints using the standard conformal approach
- the same boundary conditions —— periodic boundary conditions
- the same slicing conditions —— $\underset{\sim}{N} = 1, \quad N^i = 0, \quad \mathcal{A}^a_0 = \mathcal{A}^a_i N^i = 0$
- the same evolution scheme —— Brailovskaya predictor-corrector/iterative Crank-Nicholson
- with different set of dynamical equations
  - ADM / Ashtekar (original / strongly hyperbolic / symmetric hyperbolic)
  - λ-system, "adjusted system", $\cdots$
- The results are analyzed by monitoring the violation of constraint equations which are again compared expressed using the same (or transformed if necessary) variables.

Numerical Simulations using Ashtekar variables: Initial Data

- Metric

$$ds^2 = (-N^2 + N_x N^x)dt^2 + 2N_x dx dt + \gamma_{xx} dx^2 + \gamma_{yy} dy^2 + \gamma_{zz} dz^2 + 2\gamma_{yz} dy dz$$

- Initial data – York-O'Murchadha's Conformal Approach

Input quantities

– 3-metric $\hat{\gamma}_{ij} = \begin{pmatrix} 1 & 0 & 0 \\ & 1 + ae^{-b(x-c)^2} & 0 \\ & & 1 - ae^{-b(x-c)^2} \end{pmatrix}$ *or* $\begin{pmatrix} 1 & 0 & 0 \\ & 1 & ae^{-b(x-c)^2} \\ & & 1 \end{pmatrix}$

– tr$K = K_0$ (constant)

– TT part of the extrinsic curvature, $\hat{A}_{TT} = 0$

- Solve the Hamiltonian constraint

$$8\hat{\Delta}\psi := 8\frac{1}{\sqrt{\hat{\gamma}}}\partial_i(\hat{\gamma}^{ij}\sqrt{\hat{\gamma}}\partial_j\psi) = \hat{R}\psi + \frac{2}{3}(K_0)^2\psi^5$$

conformal transformation

$$\gamma_{ij} = \psi^4\hat{\gamma}_{ij}, \qquad K_{ij} = \frac{1}{3}\psi^4\hat{\gamma}_{ij}K_0$$

The Ashtekar formulation:

PRL **57**, 2244 (1986); PRD **36**, 1587 (1987).

- New variables

$$\mathcal{A}^a_i := \omega^{0a}_i - \frac{i}{2}\epsilon^a{}_{bc}\omega^{bc}_i = -K_{ij}E^{ja} - \frac{i}{2}\epsilon^a{}_{bc}\omega^{bc}_i \quad \text{and} \quad \tilde{E}^i_a := eE^i_a$$

- The evolution equations for a set of $(\tilde{E}^i_a, \mathcal{A}^a_i)$ are

$$\partial_t \tilde{E}^i_a = -i\mathcal{D}_j(\epsilon^{cb}{}_a \underset{\sim}{N} \tilde{E}^j_c \tilde{E}^i_b) + 2\mathcal{D}_j(N^{[j}\tilde{E}^{i]}_a) + i\mathcal{A}^b_0 \epsilon_{ab}{}^c \tilde{E}^i_c, \tag{13}$$

$$\partial_t \mathcal{A}^a_i = -i\epsilon^{ab}{}_c \underset{\sim}{N} \tilde{E}^j_b F^c_{ij} + N^j F^a_{ji} + \mathcal{D}_i \mathcal{A}^a_0 + 2\Lambda \underset{\sim}{N} \tilde{e}^a_i, \tag{14}$$

where $\mathcal{D}_j X^{ji}_a := \partial_j X^{ji}_a - i\epsilon_{ab}{}^c \mathcal{A}^b_j X^{ji}_c$, and $F^a_{ij} := 2\partial_{[i}\mathcal{A}^a_{j]} - i\epsilon^a{}_{bc}\mathcal{A}^b_i \mathcal{A}^c_j$.

- Constraint equations: (Hamiltonian, momentum and Gauss constraints)

$$\mathcal{C}^{\text{ASH}}_H := (i/2)\epsilon^{ab}{}_c \tilde{E}^i_a \tilde{E}^j_b F^c_{ij} - 2\Lambda \det\tilde{E} \approx 0, \tag{15}$$

$$\mathcal{C}^{\text{ASH}}_{Mi} := F^a_{ij}\tilde{E}^j_a \approx 0, \tag{16}$$

$$\mathcal{C}^{\text{ASH}}_{Ga} := \mathcal{D}_i \tilde{E}^i_a \approx 0. \tag{17}$$

- Gauge variables: $\underset{\sim}{N}$, N^i, and the "triad lapse" $\mathcal{A}^a_0$.

ADM 2 Ashtekar

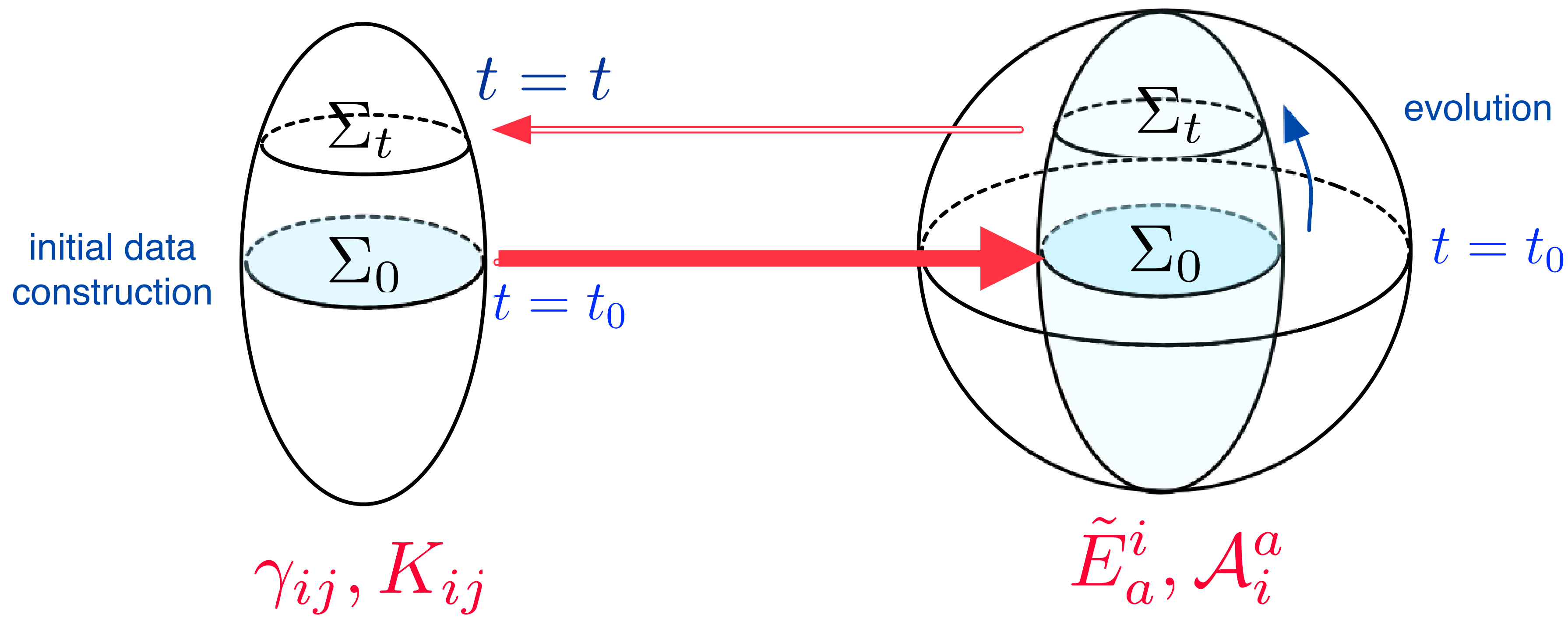

$\gamma_{ij} \Longrightarrow \tilde{E}^i_a$

1. Define a triad E^a_i from 3-metric γ_{ij}:

$$E^a_i = \begin{bmatrix} E^1_x & E^1_y & E^1_z \\ E^2_x & E^2_y & E^2_z \\ E^3_x & E^3_y & E^3_z \end{bmatrix} = \begin{bmatrix} \sqrt{\gamma_{xx}} & 0 & 0 \\ 0 & b & d \\ 0 & e & c \end{bmatrix}$$

2. inverse triad E^i_a
3. density e: $\quad e = \det E^a_i$
4. $\tilde{E}^i_a = e E^i_a$

$(\gamma_{ij}, K_{ij}) \Longrightarrow \mathcal{A}^a_i$

1. triad E^a_i
2. inverse triad E^i_a
3. connection 1-form $\omega^{bc}_i = E^{b\mu} \nabla_i E^c_\mu$

   which can be expressed

$$\omega^{IJ}_\mu = E^{\nu I} \partial_{[\mu} E^J_{\nu]} - E_{\mu K} E^{\rho I} E^{\nu J} \partial_{[\rho} E^K_{\nu]} + E^{\rho J} \partial_{[\rho} E^I_{\mu]}$$

4. $\mathcal{A}^a_i = -K_{ij} E^{ja} - \frac{i}{2} \epsilon^a{}_{bc} \omega^{bc}_i$

Ashtekar 2 ADM

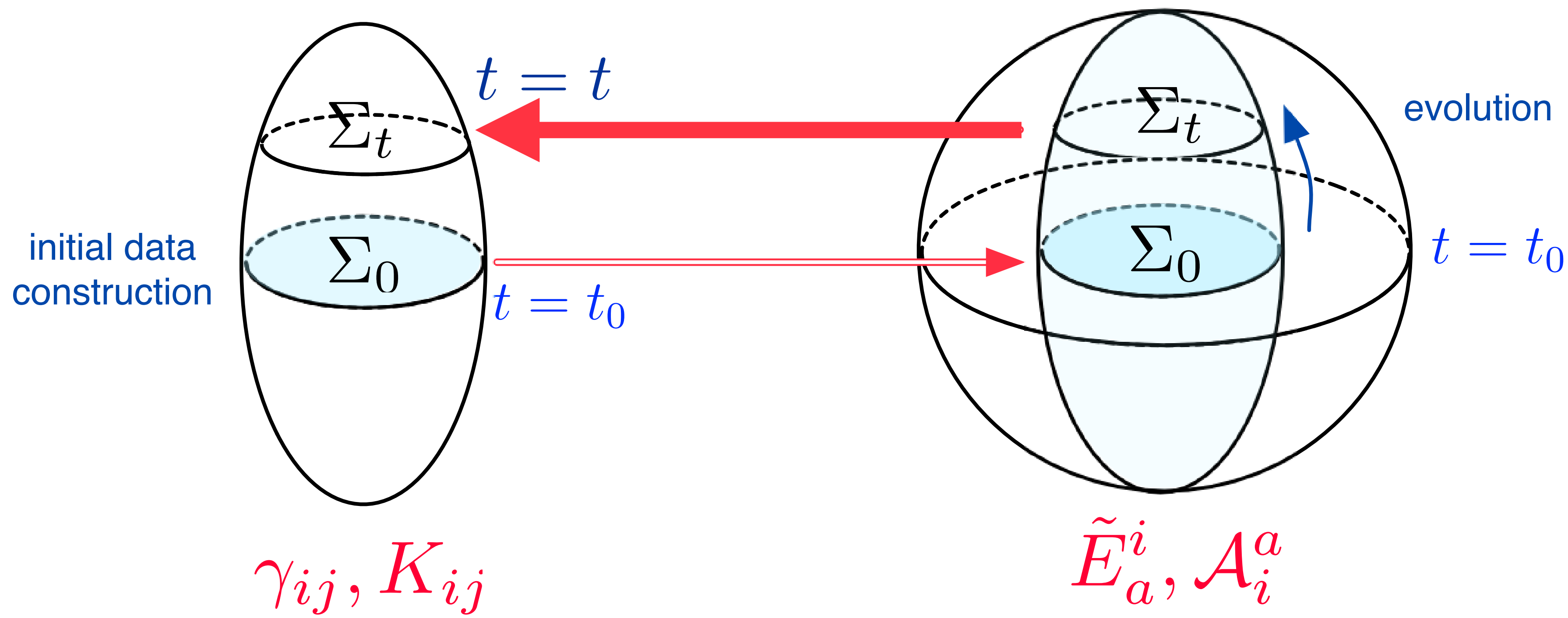

$\gamma_{ij} \Longleftarrow \tilde{E}^i_a$

1. density $e = (\det \tilde{E}^i_a)^{1/2}$
2. $\gamma^{ij} = \tilde{E}^i_a \tilde{E}^j_a / e^2$
3. γ_{ij}

$K_{ij} \Longleftarrow (\tilde{E}^i_a, \mathcal{A}^a_i)$

1. un-densitized inverse triad $E^i_a = \tilde{E}^i_a / e$
2. triad E^a_i
3. connection 1-form $\epsilon^a{}_{bc}\omega^{bc}_i$
4. $K_{ij}E^{ja} = -\mathcal{A}^a_i + \frac{i}{2}\epsilon^a{}_{bc}\omega^{bc}_i \equiv Z^a_i$, then
   $K_{ij} = Z^a_i E_{ja}$

Class. Quantum Grav. **17** (2000) 4799–4822. Printed in the UK PII: S0264-9381(00)50711-4

Hyperbolic formulations and numerical relativity: experiments using Ashtekar's connection variables

Hisa-aki Shinkai† and Gen Yoneda‡

† Centre for Gravitational Physics and Geometry, 104 Davey Laboratory, Department of Physics, The Pennsylvania State University, University Park, PA 16802-6300, USA

‡ Department of Mathematical Sciences, Waseda University, Shinjuku, Tokyo, 169-8555, Japan

E-mail: `shinkai@gravity.phys.psu.edu` and `yoneda@mn.waseda.ac.jp`

Received 3 May 2000, in final form 13 September 2000

Abstract. In order to perform accurate and stable long-time numerical integration of the Einstein equation, several hyperbolic systems have been proposed. Here we present a numerical comparison between weakly hyperbolic, strongly hyperbolic and symmetric hyperbolic systems based on Ashtekar's connection variables. The primary advantage for using this connection formulation in this experiment is that we can keep using the same dynamical variables for all levels of hyperbolicity. Our numerical code demonstrates gravitational wave propagation in plane-symmetric spacetimes, and we compare the accuracy of the simulation by monitoring the violation of the constraints. By comparing with results obtained from the weakly hyperbolic system, we observe that the strongly and symmetric hyperbolic system show better numerical performance (yield less constraint violation), but not so much difference between the latter two. Rather, we find that the symmetric hyperbolic system is not always the best in terms of numerical performance.

This study is the first to present full numerical simulations using Ashtekar's variables. We also describe our procedures in detail.

$$\partial_t \tilde{E}^i_a = -\mathrm{i}\mathcal{D}_j(\epsilon^{cb}{}_a \underset{\sim}{N} \tilde{E}^j_c \tilde{E}^i_b) + 2\mathcal{D}_j(N^{[j}\tilde{E}^{i]}_a) + \mathrm{i}\mathcal{A}^b_0 \epsilon_{ab}{}^c\, \tilde{E}^i_c,$$

$$\partial_t \mathcal{A}^a_i = -\mathrm{i}\epsilon^{ab}{}_c \underset{\sim}{N} \tilde{E}^j_b F^c_{ij} + N^j F^a_{ji} + \mathcal{D}_i \mathcal{A}^a_0,$$

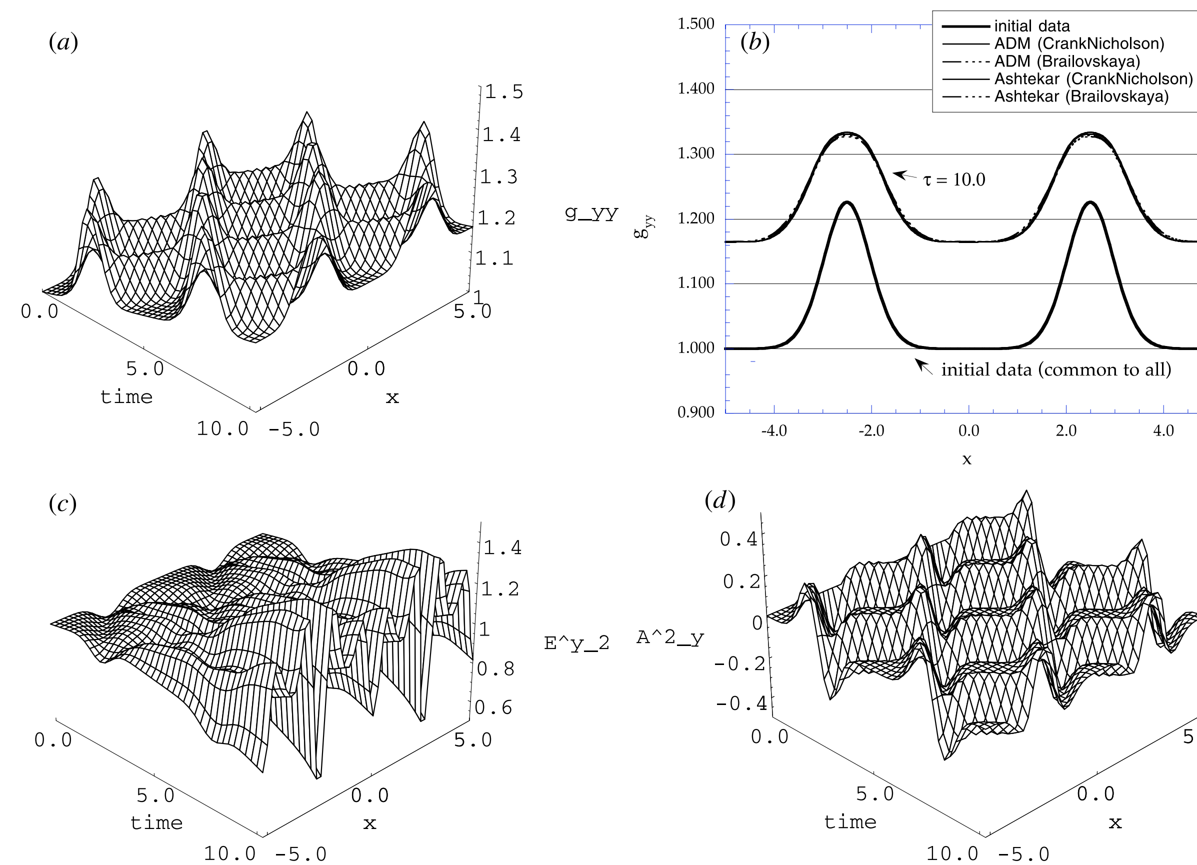

Figure 2. Images of gravitational wave propagation and comparisons of dynamical behaviour of Ashtekar's variables and ADM variables. We applied the same initial data of two +-mode pulse waves ($a = 0.2, b = 2.0, c = \pm 2.5$ in equation (21) and $K_0 = -0.025$), and the same slicing condition, the standard geodesic slicing condition ($N = 1$). (*a*) Image of the 3-metric component g_{yy} of a function of proper time τ and coordinate x. This behaviour can be seen identically both in ADM and Ashtekar evolutions, and both with the Brailovskaya and Crank–Nicholson time-integration scheme. Part (*b*) explains this fact by comparing the snapshot of g_{yy} at the same proper time slice ($\tau = 10$), where four lines at $\tau = 10$ are looked at identically. Parts (*c*) and (*d*) are of the real part of the densitized triad $\tilde{E}^y_2$, and the real part of the connection $\mathcal{A}^2_y$, respectively, obtained from the evolution of the Ashtekar variables.

Class. Quantum Grav. **18** (2001) 441–462 www.iop.org/Journals/cq PII: S0264-9381(01)15923-X

Hyperbolic formulations and numerical relativity: II. asymptotically constrained systems of Einstein equations

Gen Yoneda[1] and Hisa-aki Shinkai[2]

[1] Department of Mathematical Sciences, Waseda University, Shinjuku, Tokyo, 169-8555, Japan
[2] Centre for Gravitational Physics and Geometry, 104 Davey Lab., Department of Physics, The Pennsylvania State University, University Park, PA 16802-6300, USA

E-mail: yoneda@mn.waseda.ac.jp and shinkai@gravity.phys.psu.edu

Received 27 July 2000, in final form 13 December 2000

Adjusted-Ashtekar system works as well.

3.3.1. Adjusted system for controlling constraint violations. Here we only consider the adjusted system which controls the departures from the constraint surface. In the appendix, we present an advanced system which controls the violation of the reality condition together with a numerical demonstration.

Even if we restrict ourselves to adjusted equations of motion for $(\tilde{E}^i_a, \mathcal{A}^a_i)$ with constraint terms (no adjustment with derivatives of constraints), generally, we could adjust them as

$$\partial_t \tilde{E}^i_a = -\mathrm{i}\mathcal{D}_j(\epsilon^{cb}{}_a \underset{\sim}{N} \tilde{E}^j_c \tilde{E}^i_b) + 2\mathcal{D}_j(N^{[j}\tilde{E}^{i]}_a) + \mathrm{i}\mathcal{A}^b_0 \epsilon_{ab}{}^c \tilde{E}^i_c + X^i_a \mathcal{C}_H + Y^{ij}_a \mathcal{C}_{Mj} + P^{ib}_a \mathcal{C}_{Gb}, \tag{3.14}$$

$$\partial_t \mathcal{A}^a_i = -\mathrm{i}\epsilon^{ab}{}_c \underset{\sim}{N} \tilde{E}^j_b F^c_{ij} + N^j F^a_{ji} + \mathcal{D}_i \mathcal{A}^a_0 + \Lambda \underset{\sim}{N} \tilde{E}^a_i + Q^a_i \mathcal{C}_H + R_i{}^{ja} \mathcal{C}_{Mj} + Z^{ab}_i \mathcal{C}_{Gb}, \tag{3.15}$$

where X^i_a, Y^{ij}_a, Z^{ab}_i, P^{ib}_a, Q^a_i and R^{aj}_i are multipliers. However, in order to simplify the discussion, we restrict multipliers so as to reproduce the symmetric hyperbolic equations of motion [10, 11], i.e.

$$\begin{aligned} X &= Y = Z = 0, \\ P^{ib}_a &= \kappa_1(N^i \delta^b_a + \mathrm{i}\underset{\sim}{N}\epsilon_a{}^{bc}\tilde{E}^i_c), \\ Q^a_i &= \kappa_2(e^{-2}\underset{\sim}{N}\tilde{E}^a_i), \\ R_i{}^{ja} &= \kappa_3(\mathrm{i}e^{-2}\underset{\sim}{N}\epsilon^{ac}{}_b \tilde{E}^b_i \tilde{E}^j_c). \end{aligned} \tag{3.16}$$

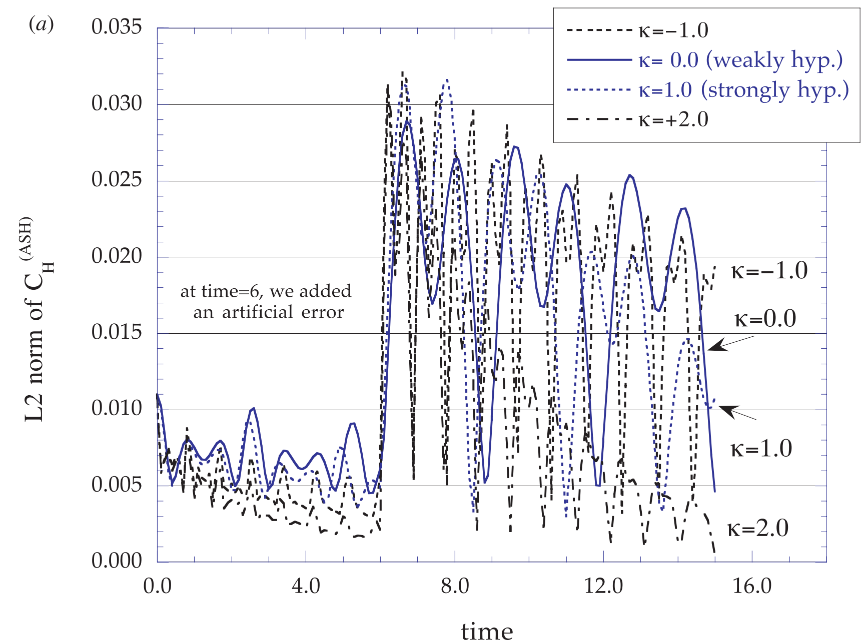

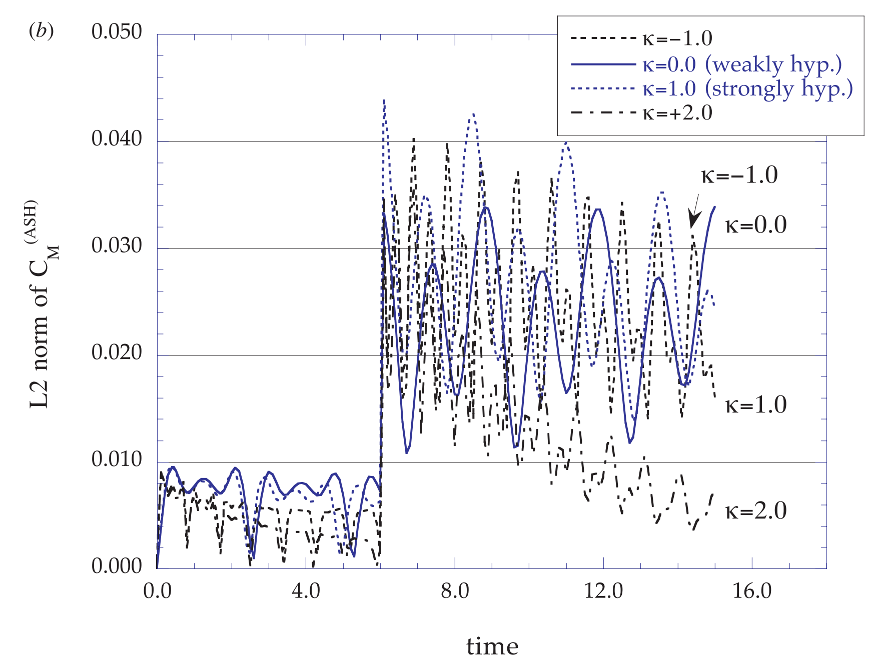

Figure 5. Demonstration of the adjusted system in the Ashtekar equation. We plot the violation of the constraint for the same model as figure 3(*b*). An artificial error term was added at $t = 6$, in the form of $\mathcal{A}^2_y \to \mathcal{A}^2_y(1 + \text{error})$, where error is + 20% as before. (*a*), (*b*) L2 norm of the Hamiltonian constraint equation, $\mathcal{C}_H$, and momentum constraint equation, $\mathcal{C}_{Mx}$, respectively. The full curve is the case of $\kappa = 0$, that is the case of 'no adjusted' original Ashtekar equation (weakly hyperbolic system). The dotted curve is for $\kappa = 1$, equivalent to the symmetric hyperbolic system. We see that the other curve ($\kappa = 2.0$) shows better performance than the symmetric hyperbolic case.